Phenotype-Based Screening of Mechanistically Annotated Compounds in Combination with Gene Expression and Pathway Analysis Identifies Candidate Drug Targets in a Human Squamous Carcinoma Cell Model

MÅRTEN FRYKNÄS,[1] LINDA RICKARDSON,[2] MALIN WICKSTRÖM,[2] SUMEER DHAR,[2] HENRIK LÖVBORG,[2] JOACHIM GULLBO,[2] PETER NYGREN,[3] MATS G. GUSTAFSSON,[1,4] ANDERS ISAKSSON,[1,2] and ROLF LARSSON[2]

The squamous cell carcinoma HeLa cell line and an epithelial cell line hTERT-RPE with a nonmalignant phenotype were interrogated for HeLa cell selectivity in response to 1267 annotated compounds representing 56 pharmacological classes. Selective cytotoxic activity was observed for 14 of these compounds dominated by cyclic adenosine monophosphate (cAMP) selective phosphodiesterase (PDE) inhibitors, which tended to span a representation of the chemical descriptor space of the library. The PDE inhibitors induced delayed cell death with features compatible with classical apoptosis. The PDE inhibitors were largely inactive when tested against a cell line panel consisting of hematological and nonsquamous epithelial phenotypes. In a genome-wide DNA microarray analysis, PDE3A and PDE2A were found to be significantly increased in HeLa cells compared to the other cell lines. The pathway analysis software PathwayAssist was subsequently used to extract a list of proteins and small molecules retrieved from Medline abstracts associated with the hit compounds. The resulting list consisted of major parts of the cAMP–protein kinase A pathway linking to ERK, P38, and AKT. This molecular network may provide a basis for further exploitation of novel candidate targets for the treatment of squamous cell carcinoma. (*Journal of Biomolecular Screening* 2006:457-468)

Key words: drug screening, annotated compound library, pathway analysis, microarray

INTRODUCTION

SQUAMOUS CELL CARCINOMA is a common histological type in head and neck cancer, cervical carcinoma, certain lung cancers, and various forms of cancer in the skin. Medical treatment of this type of cancer in the metastatic setting with standard or investigational cytotoxic drugs yields poor treatment results, and improved pharmacological treatment principles are urgently needed.[1]

Although most screening efforts for identification of new drug candidates is directed toward known or emerging molecular targets, there is a growing interest in screening based on compound-induced changes in cellular phenotypes using large and chemically diverse compound libraries.[2,3] A novel and complementary approach for cell phenotype–based screening using small organic drug molecules was recently introduced by Stockwell and coworkers.[4] The method was based on high-throughput screening (HTS) of a mechanistically annotated compound library denoted ACL.[4] The ACL library contained 2036 compounds with diverse and experimentally validated biological mechanisms. This approach was capable of not only identifying novel lead compounds with cancer phenotype selectivity but also generated testable hypotheses regarding the underlying biological mechanism.[4,5] The development of novel molecular technologies such as cDNA microarrays has made it possible to integrate gene expression and drug activity data in cell lines to identify relationships between individual genes and sensitivity or resistance to specific drugs.[6,7] We have recently successfully implemented a similar approach using a cell line panel consisting of pairs of sensitive and resistant human tumor cell lines.[8]

In the present study, the squamous cell carcinoma cell line HeLa and an epithelial cell line hTERT-RPE with a nonmalignant

[1]Department of Genetics and Pathology;
[2]Department of Medical Sciences, Division of Clinical Pharmacology;
[3]Department of Oncology, Radiology, and Clinical Immunology; and
[4]Department of Engineering Sciences, Uppsala University, S-751 85 Uppsala, Sweden.

Received Nov 29, 2005, and in revised form Jan 31, 2006. Accepted for publication Feb 27, 2006.

Journal of Biomolecular Screening 11(5); 2006
DOI: 10.1177/1087057106288048

phenotype were interrogated for carcinoma selectivity in response to 1267 compounds with known and annotated mechanisms of action. In parallel, the cell lines were also profiled for gene expression, and the results were compared with a broad panel of additional cell lines. The cell line panel represented a variety of both solid tumors and leukemias and included several drug-resistant sublines. A pathway analysis software was finally used to generate a molecular network based on Medline abstracts associated with the HeLa selective hit compounds. The cyclic adenosine monophosphate (cAMP)–protein kinase A (pkA) pathway in general and phosphodiesterase (PDE) inhibition in particular were identified as putative targets for inducing selective tumor cell apoptosis in this model.

MATERIALS AND METHODS

Cell culture

The cell lines used in this study were HeLa (squamous cell carcinoma) and hTERT-RPE (normal epithelial cell line), which were obtained from American Type Culture Collection and Clontech (Palo Alto, CA), respectively. The remaining cell line panel used has been described in detail previously[9,10] and consists of the parental cell lines RPMI 8226 (myeloma), CCRF-CEM (leukemia), NCI-H69 (small-cell lung cancer), U-937 GTB (lymphoma), ACHN (renal cell carcinoma), and the drug-resistant sublines 8226/Dox40, 8226/Dox6, 8226/LR5, 8226/CHS, CEM/VM-1, U-937 VCR, U-937 CHS, and H69AR. The sublines 8226/Dox40 and 8226/Dox6 were exposed to 0.24 and 0.06 μg/ml, respectively, of doxorubicin once a month and overexpresses Pgp/MDR1/ABCB1.[11] The 8226/LR5 subline was exposed to 1.53 μg/ml of melphalan at each change of medium, and the resistance is proposed to be associated with increased levels of glutathione as well as genes involved in cell cycle and DNA repair.[12-14] U937 VCR was continuously cultured in the presence of 10 ng/ml vincristine, and the resistance is proposed to be tubulin associated.[15] H69AR was alternately fed with drug-free medium and medium containing 0.46 μg/ml of doxorubicin and overexpresses MRP1/ABCC1.[16-18] CEM/VM-1 was cultured in drug-free medium and could be grown for 3 to 4 months without loss of resistance against teniposide, which is proposed to be associated with topoisomerase II.[19-21] U-937 CHS and RPMI 8226/CHS were selected for resistance to cyanoguanidine CHS 828 and were cultured at concentrations of 0.1 and 0.5 μM, respectively. The resistant phenotypes were stable for more than 3 mo.[10] HeLa cells were cultured in Eagle minimal essential medium supplemented with 100 mM sodium pyruvate and hTERT-RPE in modified Eagles medium nutrient mixture F-12 Ham. Both cell cultures were supplemented with 10% heat-inactivated fetal calf serum, 2 mM glutamine, 100 μg/ml streptomycin, and 100 U/ml penicillin (all from Sigma Aldrich Co., St Louis, MO) at 37° C in humidified air containing 5% CO_2. The remaining cell lines cells were grown in culture medium RPMI-1640 supplemented with 10% heat-inactivated fetal calf serum, 2 mM glutamine, 100 μg/ml streptomycin, and 100 U/ml penicillin (Sigma) under the same conditions. The resistant cell lines were tested regularly for maintained resistance to the selected drugs. Growth and morphology of all cell lines were monitored on a weekly basis.

Preparation of compounds

The LOPAC library (Sigma-Aldrich) consists of 1267 pharmacologically active compounds in 56 pharmacological classes (**Table 1**). A full description of the contents of the LOPAC library can be obtained online from the Web site http://www.medsci.uu.se/klinfarm/pharmacology/supplement.htm.

The library comes in 16 racks each containing 80 drugs dissolved in DMSO to 10 mM. The drugs were transferred to 96-well plates and were further diluted with phosphate-buffered saline (PBS) to obtain stock solutions of 100 μM from which 4 different 384-well plates for screening were prepared with final concentrations of 10 μM. The final DMSO concentrations did not exceed 1% in any of the experiments performed. In all steps, the Biomek 2000 pipetting station connected to a plate stacker carousel (Beckman Coulter Inc., Fullerton, CA) in a safety cabinet (Bigneat Inc., Hampshire, UK) was used. Dose-response plates containing the PDE inhibitors quazinone, zardaverine, and imazodan were prepared in concentrations 0.01 to 100 μM using the same robotic system. All drugs were from Sigma-Aldrich, and the plates were stored at –70° C until further use.

Fluorometric microculture cytotoxicity assay

The fluorometric microculture cytotoxicity assay (FMCA), described in detail previously,[9] is based on measurement of fluorescence generated from hydrolysis of fluorescein diacetate to fluorescein by cells with intact plasma membranes. Cells were seeded in the drug-prepared 384-well plates using the pipetting robot Precision 2000 (Bio-Tek Instruments Inc., Winooski, VT). The number of cells per well were 2500 to 5000. Two columns without drugs served as controls, and 1 column with medium only served as a blank. The plates were incubated for 72 h and then transferred to an integrated HTS SAIGAN Core System consisting of an ORCA robot (Beckman Coulter) with CO_2 incubator (Cytomat 2C; Kendro, Sollentuna, Sweden), dispenser module (Multidrop 384; Titertek, Huntsville, AL), washer module (ELx 405; Bio-Tek Instruments Inc.), delidding station, plate hotels, barcode reader (Beckman Coulter), liquid handler (Biomek 2000; Beckman Coulter), and a multipurpose reader (FLUOstar Optima; BMG Labtech GmbH, Offenburg, Germany) for automated FMCA. Quality criteria for a successful assay included a mean coefficient of variation (CV) of less than 30% in the control and a fluorescence signal in control

Table 1. Pharmacological Mechanisms of the Compounds in the LOPAC Library

Drug Class/Target	*Number of Drugs*
Adenosine	59
Adrenoreceptor	103
Angiogenesis	1
Antibiotic	29
Anticonvulsant	12
Apoptosis	11
Benzodiazepine	7
Biochemistry	46
Ca^{2+} channel	17
Calcium signaling	1
Cannabinoid	6
Cell cycle	15
Cell stress	20
Cholecystokinin	3
Cholinergic	77
Cl^- channel	3
Cyclic nucleotides	31
Cytokines and growth factors	1
Cytoskeleton and extracellular matrix	10
DNA	9
DNA metabolism	14
DNA repair	3
Dopamine	113
G protein	4
Gamma-aminobutyric acid	41
Gene regulation	1
Glutamate	88
Glycine	2
Histamine	31
Hormone	33
Imidazoline	11
Immune system	11
Intracellular calcium	7
Ion pump	16
K^+ channel	17
Leukotriene	10
Lipid	9
Lipid signaling	2
Melatonin	8
Multidrug resistance	12
Na^+ channel	17
Neurotransmission	45
Nitric oxide	37
Nootropic	3
Opioid	27
P2 receptor	14
Phosphorylation	93
Prostaglandin	24
Prostanoids	1
Serotonin	83
Somatostatin	2
Sphingolipid	4
Tachykinin	5
Thromboxane	2
Transcription	12
Vanilloid	5

wells of more than 5 times the blank. In the present study, the mean CV in the untreated control wells was 13.0%. The mean Z′ value was 59, and the mean signal-to-background ratio was 102.

Multiparametric high-content screening assays

To study the cell death characteristics of the PDE inhibitors, a multiparametric high-content screening (HCS) assay was used (HitKit™; Cellomics Inc., Pittsburgh, PA) in addition to an HCS assay for measurement of apoptosis, which has been described in detail previously.[22] The cells (1500 cells/well) were seeded into flat-bottomed 96-well plates (PerkinElmer Inc., Wellesley, MA) and were left to attach before addition of drugs. For the cytotoxicity assay, the cytotoxicity HitKit™ reagents (Cellomics Inc.) was used according to the manufacturer's instructions. The multiparameter cytotoxicity HitKit™ contains a nuclear dye, a cell permeability dye, and a lysosomal mass/pH indicator. In the apoptosis assay, FAM-DEVD-FMK (part of the CaspaTag Kit; Chemicon, Temecula, CA) at a final concentration of 20 μM was added 1 h before the end of the drug exposure to stain activated caspase-3 and partly caspase-7. The staining solution was removed, and the plates were washed twice with PBS followed by a 30-min fixation in 3.7% formaldehyde and nuclear staining with10 μM Hoechst 33342 (Sigma). Plates were then washed twice. The plates were centrifuged before each aspiration to avoid loss of cells detached due to toxic stimuli. Processed plates were kept at +4° C for up to 24 h before analysis. Plates were analyzed using the ArrayScan™ HCS software (Cellomics Inc.). The system is a computerized, automated fluorescence-imaging microscope that automatically identifies stained cells and reports the intensity and distribution of fluorescence in individual cells. Images were acquired for each fluorescence channel, using suitable filters with 20× objective. In each well, at least 800 cells were analyzed. Images and data were stored in a Microsoft SQL database for easy retrieval.

Data analysis

Small Laboratory Information and Management System (SLIMS)[5] was used for data management and analysis. Raw fluorescence data files were loaded into the SLIMS software, which calculates the percentage inhibition according to the following formula: percentage inhibition = $100 \times (x$ – negative control/positive control – negative control) – 1, where x denotes fluorescence from experimental wells. Greater than or equal to 50% inhibition in HeLa but not in hTERT-RPE was set as the criterion for qualifying as a hit compound. IC_{50} values (concentration causing 50% inhibition v. untreated control) for zardaverine, imazodan, and quazinone were calculated based on serial dilutions (0.01 to 100 μM). Structural similarity of LOPAC compounds was calculated based on a structural fingerprint consisting of binary vectors representing structures

located within the compound and that are automatically computed for each compound loaded into the program. This information was used to create self-organizing maps mapping the structural space of the compound library using default settings in SLIMS.[5]

RNA extraction

Total RNA was extracted from each cell line starting from 10^7 cells, using Trizol reagent (Invitrogen, Carlsbad, CA) according to the manufacturer's protocol. The purity of the RNA was ensured by measuring the optical density at 260 and 280 nm. The integrity of the RNA was controlled by capillary electrophoresis using a Bioanalyzer 2100 (Agilent Technologies, Palo Alto, CA). Only pure RNA (OD 260/280 >1.8) without any sign of degradation was used in the subsequent experiments.

Microarray expression analysis

RNA samples were processed and used for CodeLink™ Bioarray (GE Healthcare, Piscataway, NJ) hybridization as previously described.[23] For each CodeLink™ Bioarray, double-stranded cDNA and subsequent cRNA was synthesized from 2 µg of total RNA from each cell line using the CodeLink™ Expression Assay Kit (GE Healthcare) according to the manufacturer's instructions. In brief, biotin 11-UTP (PerkinElmer) was used in the in vitro transcription. The double-stranded cDNA was purified with the use of a QIAquick purification kit (Qiagen, Hilden, Germany). The labeled cRNA was purified using an RNeasy mini kit (Qiagen). Expression arrays used were CodeLink™ UniSet Human 20K Bioarray (GE Healthcare) containing a collection of 20,289 target probes. Bioarrays were stained with Cy5 streptavadin (GE Healthcare) and scanned using a GenePix 4000B scanner (Axon Instruments, Union City, CA). Scanned image files were analyzed with the use of CodeLink™ image and data analysis version 4.0 software (GE Healthcare), which produced both raw and median normalized hybridization signal intensities for each spot on the arrays. Normalized and background subtracted signal intensities were used in this study.

Quantitative real-time PCR validation of microarray data

Reverse transcription of 2 µg total RNA was performed with the Omniscript RT kit (Qiagen) in a volume of 20 µl using random hexamers and RNaseOUT (Invitrogen, Carlsbad, CA) according to the protocol of the manufacturer. TaqMan primers and probes were ordered as assay on demand (Applied Biosystems, Foster City, California) for 18S rRNA (product 4319413E), PDE3A (assay ID Hs01012698_m1), and PDE2A (assay ID Hs00159935_m1). Amplifications were performed in 25-µl reactions using TaqMan Universal PCR MasterMix (Applied Biosystems). All PCR reactions were performed in triplicate on the ABI PRISM 7000 Sequence Detector (Applied Biosystems) with the following thermo cycling conditions: 10 min at 95° C, followed by 40 cycles of 15 s at 95° C and 1 min at 60° C. The data were analyzed and converted into threshold cycle (C_t) values with the use of the ABI Prism 7000 software system (Applied Biosystems). The C_t values were then translated into relative cDNA copy numbers by comparison to serial dilutions. The individual expression levels were normalized to the expression of 18S rRNA for each sample.

Identification of molecular pathways

PathwayAssist is a software for visualization and exploration of biological pathways, gene regulation networks, and protein-protein interactions. PathwayAssist is supplied with ResNet molecular interaction and pathway database, which contains more than 500,000 functional links for more than 50,000 proteins, extracted from more than 5,000,000 Medline abstracts and full-length articles (ResNet update Q3 2005).

PathwayAssist v3.0 (www.ariadnegenomics.com) was used to extract a list of proteins and small molecules retrieved from Medline abstract titles, associated with the hit compound names. The list was manually curated to remove obvious artifacts generated by the automatic text mining. All molecules with 2 or more occurrences in the list were used in the subsequent pathway analysis. The complete list can be found in supplementary information at the Web site http://www.medsci.uu.se/klinfarm/pharmacology/supplement.htm. PathwayAssist was then used in 2 steps to explore the interactions between the molecules in the list. In the 1st step, the ResNet database was searched to establish direct interactions between the molecules occurring more than twice in the list, and in the 2nd step, the interacting molecules were searched for linkage to apoptosis.

RESULTS

Screening for cytotoxic activity using an annotated compound library

The HeLa and hTERT-RPE cell lines were tested for cytotoxic/antiproliferative activity in response to 1267 annotated compounds at 10 µM representing 56 pharmacological classes (**Table 1**). For the HeLa cell line, 37 of these drugs showed more than 50% inhibition (**Fig. 1**), whereas the corresponding number of drugs for hTERT-RPE was 34. Of these compounds, 14 drugs caused greater than or equal to 50% inhibition in HeLa and less than 50% inhibition in hTERT-RPE cells (**Fig. 1**). These compounds, as detailed in **Table 2**, represented different mechanistic classes, and notably, there were 6 annotated as PDE inhibitors. A self-organizing map was generated by mapping the structural space of the compound library (**Fig. 2**), and the PDE inhibitors tended to span this representation of chemical descriptor space, suggesting mechanistic

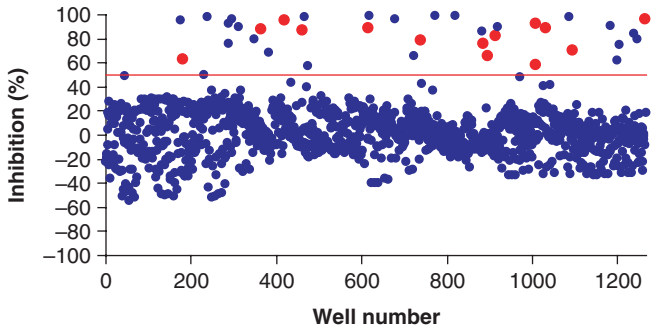

FIG. 1. Cytotoxic/antiproliferative effects of the 1267 compounds (10 µM) in the LOPAC library on HeLa cells determined by fluorometric microculture cytotoxicity assay. Blue circles denote the inhibition evoked by the compounds; red circles highlight the compounds causing greater than or equal to 50% inhibition in HeLa cells but less than 50% inhibition in hTERT cells. The red line shows the 50% inhibition cutoff used to identify the active drugs.

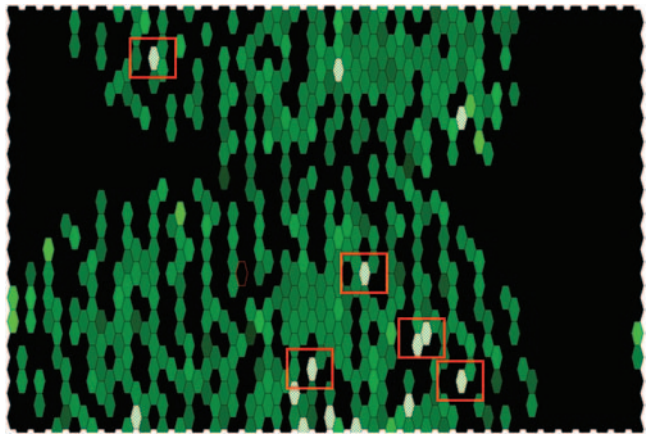

FIG. 2. Self-organizing map (SOM) generated by the Small Laboratory Information and Management System, based on all compounds in the LOPAC library. The SOM visualizes the structure-space location of hit compounds. Each node contains a collection of structurally similar compounds, and each neighboring node is more similar than nonneighboring nodes. The hits are shown in white cross-hatched nodes. The red squares indicate the location of the hit PDE inhibitor compounds. The black areas contain no compounds.

Table 2. Drugs Showing Selective Activity for HeLa Cells Compared to hTERT Cells

					% Inhibition	
Name	*Class*	*Action*	*Selectivity*	*Description*	*HeLa*	*hTERT*
DCEBIO	K^+ channel	Activator	hlK1	Activation of a basolateral membrane-located K^+ channel (hlK1)	96	23
Diphenyleneiodonium chloride	Nitric oxide	Inhibitor	eNOS	Endothelial nitric oxide synthase inhibitor	88	47
Enoximone	Cyclic nucleotides	Inhibitor	PDE III	Selective PDE III inhibitor	87	10
Imazodan	Cyclic nucleotides	Inhibitor	PDE II	Selective PDE II inhibitor	89	22
Oligomycin A	Antibiotic	Inhibitor	F0F1	Mitochondrial F0F1-ATP synthase inhibitor	76	26
Papaverine hydrochloride	Cyclic nucleotides	Inhibitor	PDE	PDE inhibitor	82	–4
Pentamidine isethionate	Glutamate	Antagonist	NMDA	NMDA glutamate receptor antagonist; neuroprotective agent; antimicrobial agent	65	24
Quazinone	Cyclic nucleotides	Inhibitor	PDE III	PDE III inhibitor	93	7
Quinacrine dihydrochloride	Neurotransmission	Inhibitor	MAO	MAO inhibitor; antimalarial	59	36
Ro 20-1724	Cyclic nucleotides	Inhibitor	PDE	Potent and selective cAMP PDE inhibitor	63	–6
Rotenone	Cell stress	Modulator	Mitochondria	Inhibitor of mitochondrial electron transport	89	34
SKF 96365	Ca^{2+} channel	Inhibitor	Calcium channel	Selective inhibitor of receptor-mediated and voltage-gated Ca^{2+} entry	71	19
Zardaverine	Cyclic nucleotides	Inhibitor	PDE III/ PDE IV	PDE III and PDE IV inhibitor	96	21
3-Methyl-6-(3-[trifluoromethyl] phenyl)-1,2,4-triazolo [4,3-b]pyridazine	Benzodiazepine	Agonist	BZ1	Selective benzodiazepine receptor (BZ1) agonist	78	5

eNOS = endothelial nitric oxide synthase; PDE = phosphodiesterase; NMDA = N-methyl-D-aspartate; MAO = monoamine oxidase; cAMP = cyclic adenosine monophosphate.

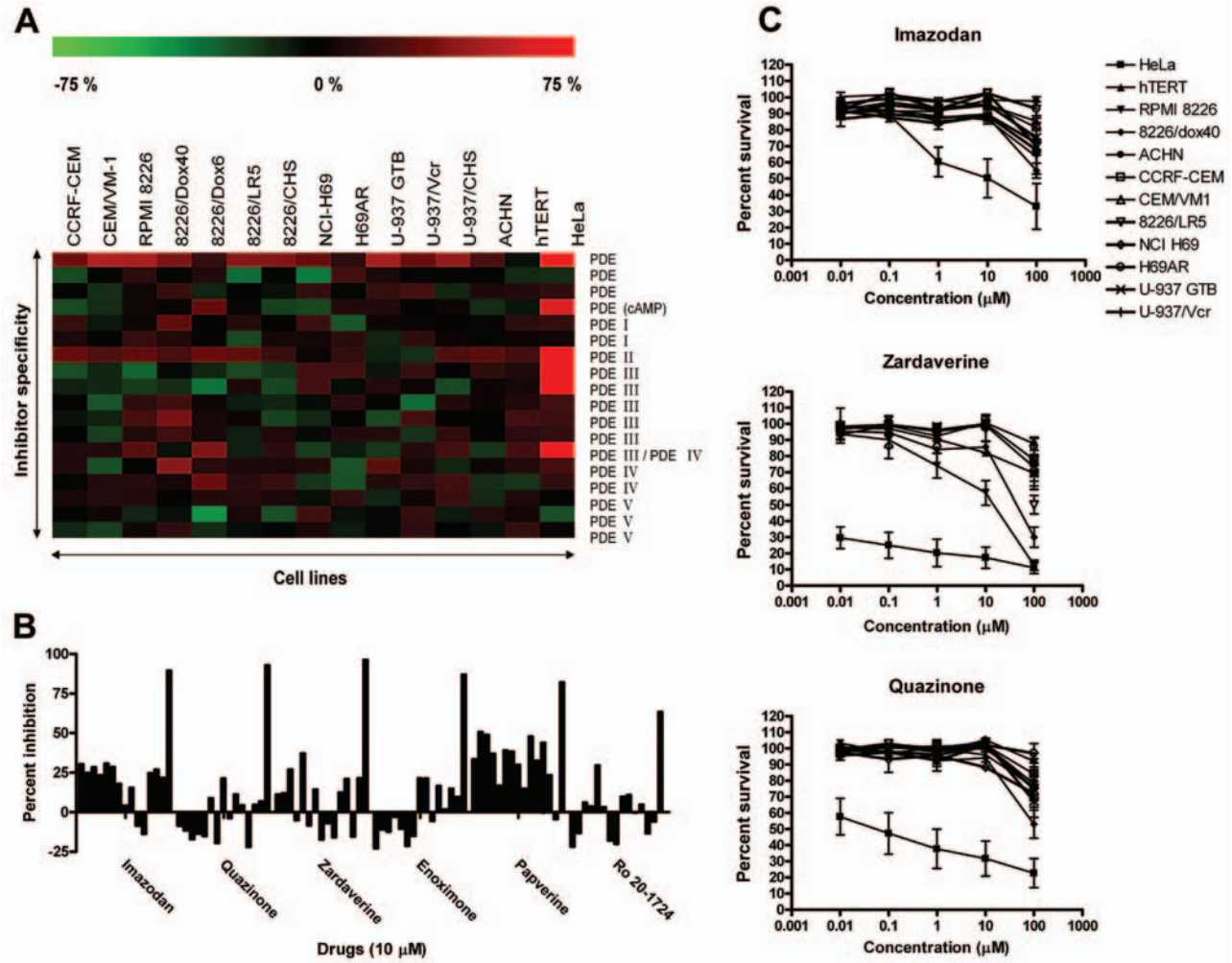

FIG. 3. The effect of phosphodiesterase (PDE) compounds on different cancer cell lines. In (**A**), a heat map of the activity of all PDE inhibitors included in the LOPAC library is shown. From the top: papaverine hydrochloride, pentoxifylline, quercetin dehydrate, Ro 20-1724, 8-methoxymethyl-3-isobutyl-1-methylxanthine, vinpocetine, imazodan, enoximone, quazinone, cilostazol, zardaverine, rolipram, ibudilast, zaprinast, T-0156, and T-1032 (all at 10 μM). (**B**) The percentage inhibition values for the HeLa hit compounds in all cell lines, in the same order as in (**A**). (**C-E**) Concentration-response curves for the PDE II inhibitor imazodan, the PDE3 inhibitor quazinone, and the PDE III/IV inhibitor zardaverine are shown for all cell lines tested using the fluorometric microculture cytotoxicity assay. The results are presented as percentage survival and expressed as mean values ± SEM for 3 independent experiments. cAMP = cyclic adenosine monophosphate.

rather than chemical similarity as the common denominator for these drugs.

The 2 cell lines were also retested in response to the library at 1 μM, and the PDE class of compounds remained more active against the HeLa cell line than hTERT cells did (not shown). Subsequently, we tested the LOPAC library at 1 and 10 μM for an additional panel of cell lines. None of the cell lines demonstrated PDE inhibitor sensitivity comparable to HeLa cells (**Figs. 3A, B**). Concentration-response analysis for the 3 most active PDE inhibitors, zardaverine, imazodan, and quazinone, confirmed the selective drug activity in HeLa cells (**Fig. 3C**). The IC_{50} values in HeLa and hTERT, respectively, were zardaverine, <0.01 μM and >100 μM; imazodan, 10 μM and >100 μM; and quazinone, 0.06 μM and >100 μM.

Microarray-based analysis of PDE mRNA expression

To elucidate the molecular basis for the PDE inhibitor hypersensitivity, microarray expression data were generated for all cell lines without drug exposure. Relative expression of all PDEs represented on the Codelink™ arrays are shown in **Figure 4A** for all cell lines. Significantly higher expression of

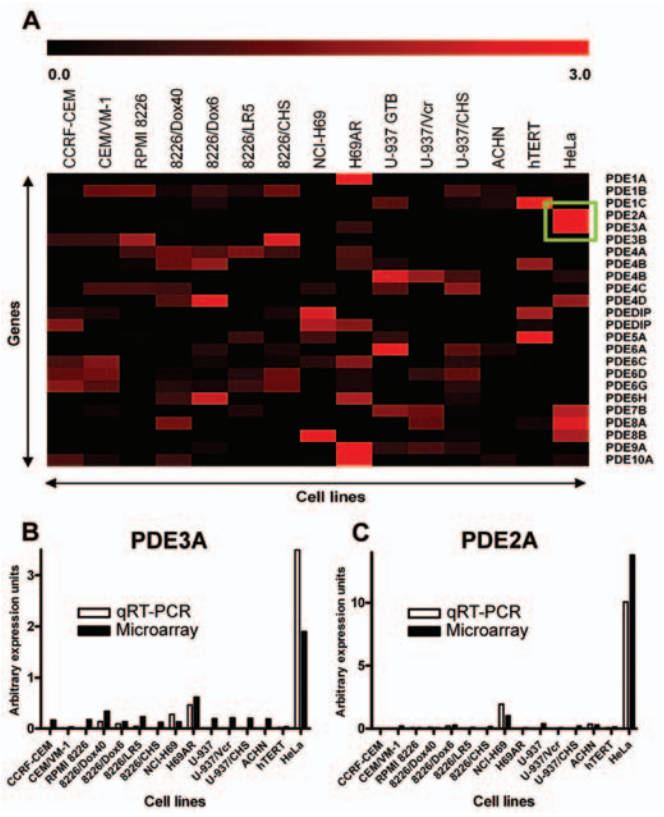

FIG. 4. The phosphodiesterase (PDE) mRNA expression in the different cell lines. Relative mRNA expression (Log_2) of all PDE genes present on the Codelink™ arrays for all cell lines displayed in a heat map (**A**). The green box highlights the expression of PDE2A and PDE3A in HeLa cells. (**B, C**) The expression of PDE3A (**B**) and PDE2A (**C**) are shown, and the corresponding quantitative real-time–PCR (qRT-PCR) data are displayed for comparison.

PDE2A and PDE3A mRNA was observed in the HeLa cell compared to the other cell lines (**Figs. 4B, C**), suggesting a molecular correlate for the differential PDE inhibitor sensitivity. The increased PDE expression was subsequently verified (correlation coefficient $r^2 > 0.9$) using quantitative real-time PCR (**Figs. 4B, C**).

Mechanistic evaluation using multiparameter analysis

Next, we profiled the 3 most active PDE inhibitors with respect to mechanism of action using multiparameter analysis with ArrayScan II (**Fig. 5**). The activity of zardaverine on growth and viability were delayed in time with little or no effect observable at 24 h (**Figs. 5A, B**). At 48 to 72 h, there was a gradual decrease in cell density and a parallel increase in caspase-3 activity and DNA fragmentation (**Figs. 5C-F**). The increase in DNA fragmentation and caspase activation preceded the increase in cell membrane permeability, which is compatible with classical apoptosis (**Figs. 5B, E-F**). Similar effects were obtained for imazodan and quazinone, which are summarized in bar graphs for data obtained at 10 µM for both drugs (**Figs. 5G, H**). The dissimilarity in cytotoxic effect after exposure of 0.01 µM zardaverine measured with ArrayScan and FMCA may be explained by different experimental settings (96- v. 384-well format, cell densities and/or assay end points used).

Pathway analysis

To further explore possible mechanisms, the pathway analysis software PathwayAssist was used to extract a list, retrieved from PubMed abstract titles, of proteins and small molecules associated with the hit compound names. Molecules with 2 or more occurrences in the list are shown in **Table 3**. PathwayAssist was then used to explore the interactions between the molecules in the list and their relation to apoptosis (**Fig. 6**). The resulting network consisted of major parts of the cAMP-pKA pathway and linking to other signaling molecules such as ERK, P38, and AKT.

DISCUSSION

In the present study, we have taken advantage of an annotated compound library to probe for phenotype selective activity for squamous carcinoma HeLa cells. There was a striking enrichment of PDE inhibitors among the HeLa selective hit compounds. PDEs, which hydrolyze the intracellular 2nd-messenger cAMP and cyclic guanosine monophosphate (cGMP) to their corresponding monophosphates, play an important role in signal transduction and are involved in different cellular processes including cell differentiation and apoptosis.[24,25] There are at least 11 PDE families, and cAMP is hydrolyzed specifically by PDE2, PDE3, PDE4, and PDE8, whereas cGMP is hydrolyzed preferentially by PDE5 and PDE6.[24,25] Intracellular concentrations of the cyclic nucleotides are regulated by the balance between adenylate cyclase/guanylate cyclase activity and the corresponding PDE activity. The effect of increased concentrations of cAMP or cGMP is in many cases mediated by pkA and B (pkG)–activated pathways, respectively.[25]

PDE inhibitors targeting the cGMP-pkG pathway have previously been identified as a potentially useful class of anticancer agents.[26] Exisulind, a derivative of the nonsteroidal anti-inflammatory drug sulindac as well as other PDE5 inhibitors, has been shown to induce apoptosis and growth inhibition in a variety of epithelial tumor cell types via cGMP-selective PDE inhibition, and the former drug is also under active clinical development for cancer treatment.[26]

The active PDE inhibitors of the present study also induced delayed cell death with morphological and biochemical hallmarks of apoptosis. However, in contrast, cAMP-specific PDEs rather than cGMP-specific isoforms produced this effect.

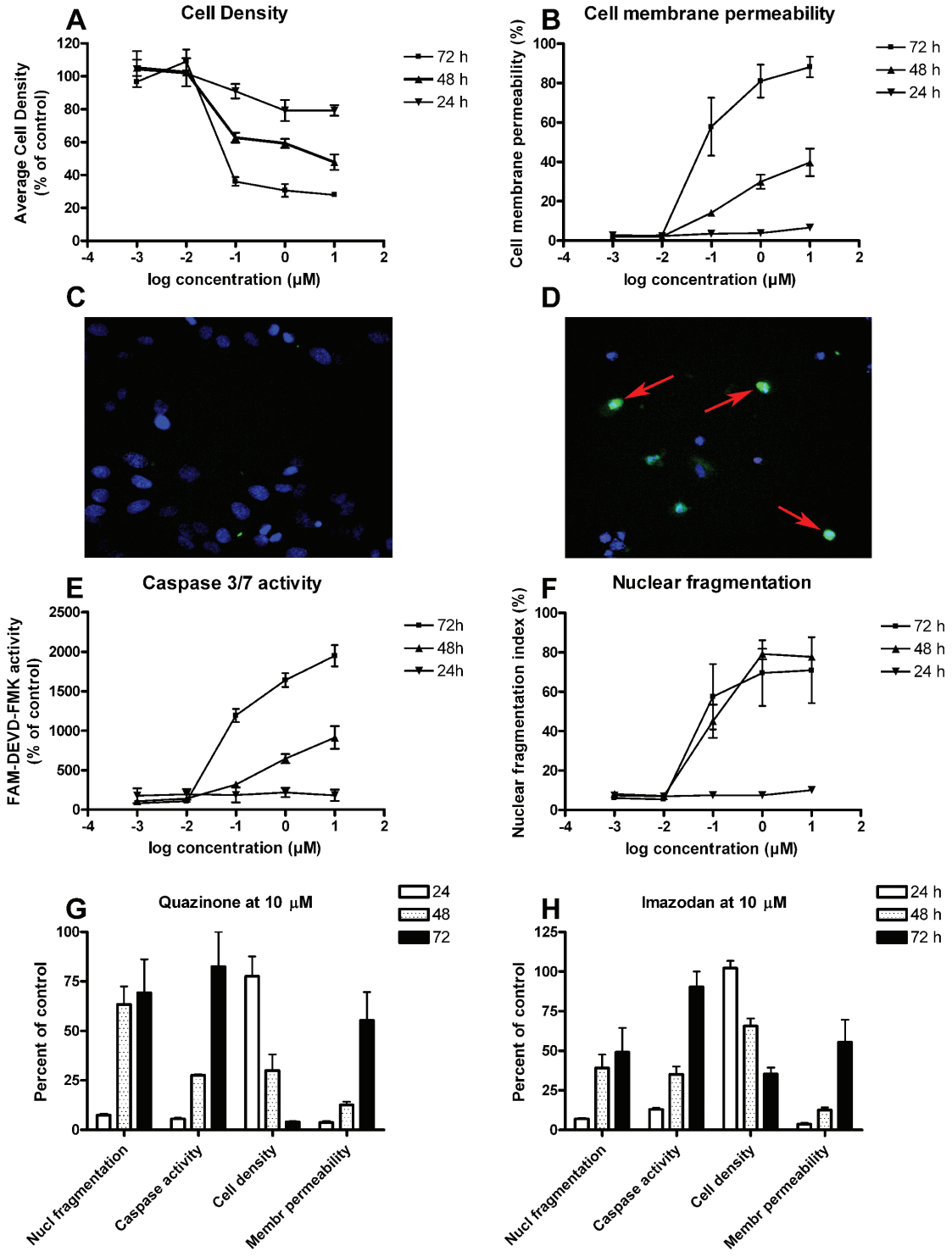

FIG. 5. Mechanistic profiling of the activity in the HeLa cell line using ArrayScan II. The effect of zardaverine on average cell density over time (24-72 h) and cell membrane permeability is shown in (**A**) and (**B**). Cell density (**A**) and cell membrane permeability (**B**) are expressed as the percentage of the untreated control. (**C, D**) Photomicrographs of zardaverine-treated cells (72 h; **D**) versus control (**C**) stained by Hoechst 3342 and CaspaTag are shown, and the caspase-positive cells are indicated with arrows. (**E, F**) Caspase 3/7 activity and nuclear fragmentation in zardaverine-treated cells. Caspase activity measured using FAM-DEVD-FMK (**E**) and nuclear fragmentation (**F**) is expressed in percentage of untreated control. (**G, H**) The above parameters are estimated and summarized in response to 10 μM quazinone and imazodan, respectively. The results are presented as mean values ± SEM for 3 independent experiments.

Table 3. Mechanisms for Selective Drug Activity Identified by PathwayAssist PubMed Search

Mechanism	*Class*	*Number*
Phosphodiesterase	Functional class	13
Ca^{2+}	Small molecule	12
Cyclic AMP	Small molecule	9
Nitric oxide	Small molecule	8
Reactive oxygen species	Small molecule	8
Cyclic nucleotide phosphodiesterase	Protein	6
NADPH-oxidase	Functional class	6
Angiotensin II	Protein	4
ERK1	Protein	4
Hydrogen peroxide	Small molecule	4
MAPK	Functional class	4
Protein kinase A	Functional class	4
Arachidonic acid	Small molecule	3
ATP	Small molecule	3
ATPase	Functional class	3
β adrenoceptor	Functional class	3
Glucose	Small molecule	3
Norepinephrine	Small molecule	3
p38 MAPK	Protein	3
Adenosine	Small molecule	2
Akt	Protein	2
cAMP-specific phosphodiesterase	Functional class	2
Complex I	Protein	2
Cytochrome c	Small molecule	2
Cytochrome c oxidase	Complex	2
Endothelin-1	Protein	2
eNOS	Protein	2
F1FO-ATPase	Protein	2
Glutathione	Small molecule	2
H_2O_2	Small molecule	2
ICAM-1	Protein	2
JAK	Functional class	2
NADPH	Small molecule	2
Oxygen	Small molecule	2
PKC-δ	Protein	2
Prostacyclin	Small molecule	2
Proteasome	Complex	2
PKC	Functional class	2
Superoxide anion	Small molecule	2
TGF-β1	Protein	2

MAPK = mitogen-activated protein kinase; ATP = adenosine triphosphate; cAMP = cyclic adenosine monophosphate; eNOS = endothelial nitric oxide synthase; NADPH = nicotinamide adenosine dinucleotide phosphate; PKC = protein kinase C; TGF = transforming growth factor. Each hit compound was searched for association to small molecules, proteins, or functional classes in PubMed abstract titles. The classification into groups was automatically performed by the software.

PDE4, a cAMP-specific isoform, has been shown to induce apoptosis in lymphoid cells but is not proapoptotic in most epithelial-derived tumor cells.[27,28] In the presently used HeLa model, on the other hand, PDE2 and PDE3 in addition to PDE4 inhibitors were found to be potent inducers of apoptosis. Indeed, the PDE2 and PDE3 genes were clearly overexpressed in HeLa cells and indicate the potential importance for this cell type to control cAMP levels by these enzymes to preserve structural integrity and the ability to maintain cell survival and proliferation.

When enriched mechanisms among the hit compounds were retrieved from the literature by PathwayAssist, many of these were related to the cAMP-pkA pathway. In addition, other signaling molecules including nitric oxide (NO), Ca^{2+}, ERK, and P38 could also be linked to the hit compounds. Inducible nitric oxide (iNOS) is a gene controlled by the cAMP-pkA signaling machinery, and iNOS-generated NO has been implicated in various cellular processes including cell proliferation and cell death.[29] PDE inhibitors can influence iNOS activation, and the modulation ranges from strong suppression to marked enhancement of NO release depending on cell type.[29]

The interaction between calcium and cAMP pathways is highly complex and can occur at multiple levels of the 2 signaling pathways, and the extent and linking of pathway crosstalk differ widely depending on cell type.[30] However, in many nonexcitable cells, cAMP has been shown to inhibit release of calcium from intracellular stores and to stimulate calcium efflux.[30] The increased PDE3 and PDE expression may thus help, not only in controlling cellular levels of cAMP but also indirectly in preventing potentially proapoptotic levels of calcium to be reached. The cAMP-pkA system may also regulate mitogen-activated protein kinase signaling.[31-34] The cAMP-pkA–mediated activation of both ERK and p38 has been reported to lead to inhibition of cell growth and induction of apoptosis.[30-32,34] The molecular network obtained here thus provides a comprehensive framework of testable hypotheses for the induction of cell death in cAMP-dependent tumor types.

Whether the increased PDE sensitivity of the HeLa model is a general phenomenon for malignant tumors derived from squamous epithelium is not clear. However, in a model of squamous cell head and neck cancer (KB cell line), PDE3 activity was detected, and a PDE3-specific inhibitor could inhibit cell growth.[35] Moreover, when normal keratinocytes were compared to their malignant counterparts, the latter overexpressed PDE, and PDE inhibition induced apoptosis selectively in these cells, supporting a role for cAMP-pkA pathway as an important regulator for growth and viability in squamous epithelial cancer.[36] Thus, PDE inhibition might be a worthwhile target to exploit in drug development for treatment of squamous cell carcinoma.

Genomics-based target identification and screening using cell-free systems is currently the dominating principle in anticancer drug development. As a complement to these approaches, the use of annotated compound libraries in phenotype-based screening may provide some distinct advantages. Because annotated libraries represent a large-scale collection of compounds with diverse and experimentally validated biological mechanisms, the approach is capable of identifying compounds selectively affecting specific cellular phenotypes using different

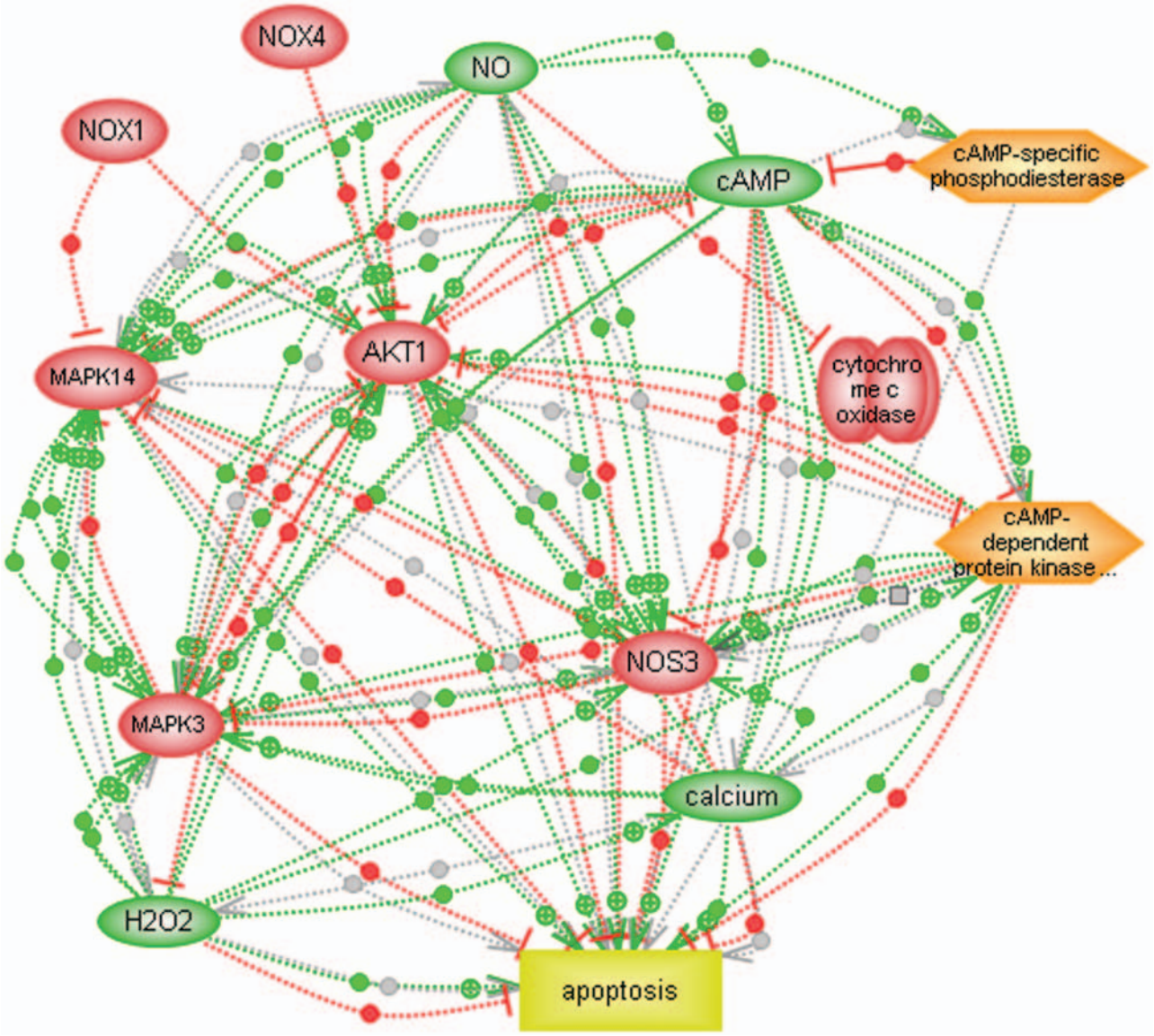

FIG. 6. Analysis of molecular interactions using PathwayAssist. The network for molecules associated with hit-list compounds is shown. Green lines indicate positive effects, red lines indicate inhibition, and gray lines indicate interactions with unknown effect. The network is accessible as supplementary information and can be downloaded from http://www.medsci.uu.se/klinfarm/pharmacology/supplement.htm. The connections are clickable (dots on lines) to access hyperlinks to the PubMed references on which the networks are based. Clicking on the nodes provides hyperlinks to several gene and protein databases including HUGO, Locus Link, and Swissprot for the particular protein.

model systems and assays as well as generating hypotheses regarding the underlying biological mechanism. Information on enriched biological mechanisms among the hit compounds can also be retrieved by automated online Medline text-mining software, as demonstrated in the present study, and this can also to some extent be performed within the SLIMS package using a downloaded version of Medline.[5] Furthermore, for many drugs, pharmacodynamic and safety information in humans already exists, making the road to clinical proof of concept testing considerably shorter.

In conclusion, in the HeLa model of squamous cell carcinoma, the cAMP-pkA pathway in general and PDE inhibition in particular were identified as drugable targets for inducing selective tumor cell apoptosis. Identification of phenotypic selectivity of drug action using annotated compound libraries may provide both new mechanistic insights in drug resistance

and a basis for new therapeutic approaches for drug-resistant malignancies.

ACKNOWLEDGMENTS

The skillful technical assistance of Christina Leek, Lena Lenhammar, and Maria Rydåker is gratefully acknowledged. This study was supported by the Swedish Cancer Society, the Swedish Research Council, the Lions Cancer Research Fund, Beijer Foundation, Wallenberg Consortium North, Marcus Borgström Foundation, Swedish Society for Medical Research, Göran Gustafsson Foundation, Carl Tryggers Foundation, and Swedish Knowledge Foundation.

REFERENCES

1. Nygren P: What is cancer chemotherapy? *Acta Oncol* 2001;40:166-174.
2. Posner BA: High-throughput screening-driven lead discovery: meeting the challenges of finding new therapeutics. *Curr Opin Drug Discov Devel* 2005;8:487-494.
3. Hart CP: Finding the target after screening the phenotype. *Drug Discov Today* 2005;10:513-519.
4. Root DE, Flaherty SP, Kelley BP, Stockwell BR: Biological mechanism profiling using an annotated compound library. *Chem Biol* 2003;10: 881-892.
5. Kelley BP, Lunn MR, Root DE, Flaherty SP, Martino AM, Stockwell BR: A flexible data analysis tool for chemical genetic screens. *Chem Biol* 2004;11:1495-1503.
6. Scherf U, Ross DT, Waltham M, Smith LH, Lee JK, Tanabe L, et al: A gene expression database for the molecular pharmacology of cancer. *Nat Genet* 2000;24:236-244.
7. Dan S, Tsunoda T, Kitahara O, Yanagawa R, Zembutsu H, Katagiri T, et al: An integrated database of chemosensitivity to 55 anticancer drugs and gene expression profiles of 39 human cancer cell lines. *Cancer Res* 2002;62:1139-1147.
8. Rickardson L, Fryknas M, Dhar S, Lovborg H, Gullbo J, Rydaker M, et al: Identification of molecular mechanisms for cellular drug resistance by combining drug activity and gene expression profiles. *Br J Cancer* 2005;93:483-492.
9. Dhar S, Nygren P, Csoka K, Botling J, Nilsson K, Larsson R: Anticancer drug characterisation using a human cell line panel representing defined types of drug resistance. *Br J Cancer* 1996;74:888-896.
10. Gullbo J, Lovborg H, Dhar S, Lukinius A, Oberg F, Nilsson K, et al: Development and characterization of two human tumor sublines expressing high-grade resistance to the cyanoguanidine CHS 828. *Anticancer Drugs* 2004;15:45-54.
11. Dalton WS, Durie BG, Alberts DS, Gerlach JH, Cress AE: Characterization of a new drug-resistant human myeloma cell line that expresses P-glycoprotein. *Cancer Res* 1986;46:5125-5130.
12. Bellamy WT, Dalton WS, Gleason MC, Grogan TM, Trent JM: Development and characterization of a melphalan-resistant human multiple myeloma cell line. *Cancer Res* 1991;51:995-1002.
13. Mulcahy RT, Bailey HH, Gipp JJ: Up-regulation of gamma-glutamylcysteine synthetase activity in melphalan-resistant human multiple myeloma cells expressing increased glutathione levels. *Cancer Chemother Pharmacol* 1994;34:67-71.
14. Hazlehurst LA, Enkemann SA, Beam CA, Argilagos RF, Painter J, Shain KH, et al: Genotypic and phenotypic comparisons of de novo and acquired melphalan resistance in an isogenic multiple myeloma cell line model. *Cancer Res* 2003;63:7900-7906.
15. Botling J, Liminga G, Larsson R, Nygren P, Nilsson K: Development of vincristine resistance and increased sensitivity to cyclosporin A and verapamil in the human U-937 lymphoma cell line without overexpression of the 170-kDa P-glycoprotein. *Int J Cancer* 1994;58:269-274.
16. Mirski SE, Gerlach JH, Cole SP: Multidrug resistance in a human small cell lung cancer cell line selected in adriamycin. *Cancer Res* 1987; 47:2594-2598.
17. Cole SP, Bhardwaj G, Gerlach JH, Mackie JE, Grant CE, Almquist KC, et al: Overexpression of a transporter gene in a multidrug-resistant human lung cancer cell line. *Science* 1992;258:1650-1654.
18. Slovak ML, Ho JP, Bhardwaj G, Kurz EU, Deeley RG, Cole SP: Localization of a novel multidrug resistance-associated gene in the HT1080/DR4 and H69AR human tumor cell lines. *Cancer Res* 1993;53:3221-3225.
19. Danks MK, Yalowich JC, Beck WT: Atypical multiple drug resistance in a human leukemic cell line selected for resistance to teniposide (VM-26). *Cancer Res* 1987;47:1297-1301.
20. Danks MK, Schmidt CA, Cirtain MC, Suttle DP, Beck WT: Altered catalytic activity of and DNA cleavage by DNA topoisomerase II from human leukemic cells selected for resistance to VM-26. *Biochemistry* 1988;27:8861-8869.
21. Mao Y, Yu C, Hsieh TS, Nitiss JL, Liu AA, Wang H, et al: Mutations of human topoisomerase II alpha affecting multidrug resistance and sensitivity. *Biochemistry* 1999;38:10793-10800.
22. Lovborg H, Nygren P, Larsson R: Multiparametric evaluation of apoptosis: effects of standard cytotoxic agents and the cyanoguanidine CHS 828. *Mol Cancer Ther* 2004;3:521-526.
23. Redmond DE Jr, Zhao JL, Randall JD, Eklund AC, Eusebi LO, Roth RH, et al: Spatiotemporal patterns of gene expression during fetal monkey brain development. *Brain Res Dev Brain Res* 2003;146:99-106.
24. Lugnier C: Cyclic nucleotide phosphodiesterase (PDE) superfamily: a new target for the development of specific therapeutic agents. *Pharmacol Ther* 2006;109:366-398.
25. Essayan DM: Cyclic nucleotide phosphodiesterases. *J Allergy Clin Immunol* 2001;108:671-680.
26. Thompson WJ, Piazza GA, Li H, Liu L, Fetter J, Zhu B, et al: Exisulind induction of apoptosis involves guanosine 3′,5′-cyclic monophosphate phosphodiesterase inhibition, protein kinase G activation, and attenuated beta-catenin. *Cancer Res* 2000;60:3338-3342.
27. Tiwari S, Dong H, Kim EJ, Weintraub L, Epstein PM, Lerner A: Type 4 cAMP phosphodiesterase (PDE4) inhibitors augment glucocorticoid-mediated apoptosis in B cell chronic lymphocytic leukemia (B-CLL) in the absence of exogenous adenylyl cyclase stimulation. *Biochem Pharmacol* 2005;69:473-483.
28. Lerner A, Kim DH, Lee R: The cAMP signaling pathway as a therapeutic target in lymphoid malignancies. *Leuk Lymphoma* 2000;37:39-51.
29. Markovic M, Miljkovic D, Trajkovic V: Regulation of inducible nitric oxide synthase by cAMP-elevating phospho-diesterase inhibitors. *Curr Drug Targets Inflamm Allergy* 2003;2:63-79.
30. Bruce JI, Straub SV, Yule DI: Crosstalk between cAMP and Ca2+ signaling in non-excitable cells. *Cell Calcium* 2003;34:431-444.
31. Reshkin SJ, Bellizzi A, Cardone RA, Tommasino M, Casavola V, Paradiso A: Paclitaxel induces apoptosis via protein kinase A- and p38 mitogen-activated protein-dependent inhibition of the Na+/H+ exchanger

(NHE) NHE isoform 1 in human breast cancer cells. *Clin Cancer Res* 2003;9:2366-2373.
32. Stork PJ, Schmitt JM: Crosstalk between cAMP and MAP kinase signaling in the regulation of cell proliferation. *Trends Cell Biol* 2002;12: 258-266.
33. Ahn YH, Jung JM, Hong SH: 8-Chloro-cyclic AMP-induced growth inhibition and apoptosis is mediated by p38 mitogen-activated protein kinase activation in HL60 cells. *Cancer Res* 2005;65:4896-4901.
34. MacKenzie SJ, Houslay MD: Action of rolipram on specific PDE4 cAMP phosphodiesterase isoforms and on the phosphorylation of cAMP-response-element-binding protein (CREB) and p38 mitogen-activated protein (MAP) kinase in U937 monocytic cells. *Biochem J* 2000;347:571-578.
35. Shimizu K, Murata T, Okumura K, Manganiello VC, Tagawa T: Expression and role of phosphodiesterase 3 in human squamous cell carcinoma KB cells. *Anticancer Drugs* 2002;13:875-880.
36. Marko D, Romanakis K, Zankl H, Furstenberger G, Steinbauer B, Eisenbrand G: Induction of apoptosis by an inhibitor of cAMP-specific PDE in malignant murine carcinoma cells overexpressing PDE activity in comparison to their nonmalignant counterparts. *Cell Biochem Biophys* 1998;28:75-101.

Address reprint requests to:
Rolf Larsson
Department of Medical Sciences
Division of Clinical Pharmacology
Uppsala University
S-751 85 Uppsala, Sweden

E-mail: rolf.larsson@medsci.uu.se